Interannual variability of air-sea O_2 fluxes and the determination of CO_2 sinks using atmospheric O_2/N_2

Galen A. McKinley,[1] Michael J. Follows, and John Marshall

Department of Earth, Atmospheric and Planetary Sciences, Massachusetts Institute of Technology, Cambridge, Massachusetts, USA

Song-Miao Fan

Atmospheric and Ocean Sciences Program, Princeton University, Princeton, New Jersey, USA

Received 8 August 2002; accepted 18 October 2002; published 1 February 2003.

[1] Motivated by the use of atmospheric O_2/N_2 to determine CO_2 sinks under the assumption of negligible interannual variability in air-sea O_2 fluxes, we examine interannual fluctuations of the global air-sea flux of O_2 during the period 1980–1998 using a global ocean circulation and biogeochemistry model along with an atmospheric transport model. It is found that both the El Niño/Southern Oscillation (ENSO) cycle and wintertime convection in the North Atlantic are primary drivers of global air-sea oxygen flux interannual variability. Model estimated extremes of O_2 flux variability are $-70/+100 \times 10^{12}$ mol/yr (Tmol/yr), where positive fluxes are to the atmosphere. O_2/N_2 variability could cause an up to ±1.0 PgC/yr error in estimates of interannual variability in land and ocean CO_2 sinks derived from atmospheric O_2/N_2 observations. *INDEX TERMS:* 0312 Atmospheric Composition and Structure: Air/sea constituent fluxes (3339, 4504); 4806 Oceanography: Biological and Chemical: Carbon cycling; 1615 Global Change: Biogeochemical processes (4805); 4215 Oceanography: General: Climate and interannual variability (3309); 4255 Oceanography: General: Numerical modeling. **Citation:** McKinley, G. A., M. J. Follows, J. Marshall, and S.-M. Fan, Interannual variability of air-sea O_2 fluxes and the determination of CO_2 sinks using atmospheric O_2/N_2, *Geophys. Res. Lett.*, *30*(3), 1101, doi:10.1029/2002GL016044, 2003.

1. Introduction

[2] Timeseries measurements of atmospheric O_2/N_2 have allowed significant advancement in quantification of the global carbon cycle. Measurements of decreasing O_2/N_2 have been combined with observations of the CO_2 increase to estimate the mean land and ocean sinks as well as their interannual variability in the 1990's [*Manning*, 2001; *Battle et al.*, 2000; *Keeling et al.*, 1996; *Bender et al.*, 1996]. In these studies, CO_2 sinks into the terrestrial biota (B) and ocean (O) are estimated from atmospheric data by making use of the global atmospheric carbon and oxygen budgets:

$$\Delta CO_2 = F - O - B \quad (1)$$

$$\Delta O_2 = \alpha_F F - \alpha_B B \quad (2)$$

[3] Here, ΔCO_2 (ΔO_2) is the observed global change in the atmospheric CO_2 (O_2) concentration, F is the global source of CO_2 due to the burning of fossil fuels and cement manufacture. The factor α_F is the O_2:C molar ratio describing O_2 utilization and CO_2 production during fossil fuel burning and α_B is the O_2:C ratio for O_2 production and CO_2 utilization during terrestrial photosynthesis. ΔO_2 is measured as O_2/N_2 in the atmosphere [*Manning*, 2001; *Keeling et al.*, 1996; *Bender et al.*, 1996]. Equations (1) and (2) assume that the global atmospheric oxygen concentration can be simply described by a terrestrial photosynthetic source and a fossil fuel combustion sink over the time period of interest. For this reason equation (2) has no term representing the air-sea O_2 flux. This simplification has usually been made for long-term fluxes, however, evidence exists that variability of air-sea fluxes of O_2 may not be negligible on interannual or longer timescales, [*Bender et al.*, 1996; *McKinley et al.*, 2000]. Further, evidence for significant variability in the ocean's physical and biogeochemical state across the globe [*Bates*, 2001; *Dickson et al.*, 1996; *McPhaden et al.*, 1998], combined with the rapid air-sea exchange timescale of O_2, indicates that global air - sea O_2 flux variability may be substantial. We use a biogeochemical ocean model to examine possible driving mechanisms and to begin to quantify air-sea O_2 flux variability on the global scale.

[4] The offline biogeochemical model is based on the MITgcm [*Marshall et al.*, 1997a, 1997b] that was configured and integrated at the Jet Propulsion Laboratory [*Lee et al.*, 2002]. The resolution of the physical model is 1° in longitude and varies from 0.3° latitudinal resolution in the tropics to 1° at high latitudes. There are 47 vertical levels. The biogeochemical model is forced with 10 day-average fields from the physical model which was forced with 12 hourly winds and heat and freshwater fluxes from the NCEP reanalysis for the period 1980–1998. The model captures the major features of the mean ocean circulation and its variability. However, comparisons of model upper ocean variability to observations indicate that the model significantly under-represents physical variability [*McKinley*, 2002]. This under-representation suggests that the O_2 air-sea flux variability estimates made here are likely to be lower bounds. A simplified parameterization for particle export of phosphorus in particles is used: $\frac{\partial P}{\partial t} = -\alpha(x,y)\frac{I}{I+I_o}\frac{P}{P+P_o}$. Light (I(x, z, t)) and nutrient limitation are included explicitly. All other influences on export are included in a spatially inhomogeneous export factor, α, which varies over 14 basin-scale regions such that the mean nutrient concentration in each region remains close to the observed climatology over the course of the 19 year model run [*McKinley*, 2002]. The sinking

[1] Now at Instituto Nacional de Ecología, México DF, México.

0094-8276/03/2002GL016044$05.00

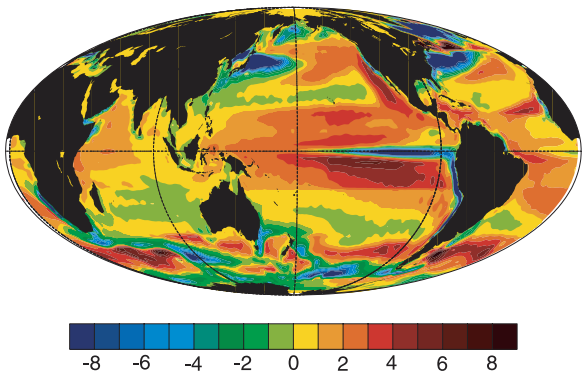

Figure 1. Model mean O_2 flux in mol/m^2/yr, positive to the atmosphere.

particle flux at all depths is parameterized using an exponential profile with a scale height of 400m, the divergence of which provides the remineralization source of P. Biological transformations are assumed to impact O_2 in Redfield proportion to changes in P [*Anderson and Sarmiento*, 1994]. Air-sea exchange of O_2 is parameterized following *Wanninkhof* [1992] using the solubility from *Weiss* [1970]. In the gas exchange calculation, we use 12 hour-equivalent winds calculated according to *Boutin and Etcheto* [1995]. Air-sea fluxes are reduced in the presence of sea ice, proportional to ice coverage. Atmospheric O_2 is held at a constant concentration of 20.946 pph. The offline biogeochemical model is run only in the upper ocean (0–1265 m), and relaxation to climatological tracer concentrations occurs over the three deepest layers (965–1265 m). P and O_2 fields are initialized with climatological values from *Conkright et al.* [1998]. An annual climatology of the 19 years (1980–1998) of physical model fields was used to force the biogeochemical model for 22 years of spinup before applying the interannually varying fields, with 2-hour timestep, to the tracers.

2. Results

[5] The mean air-sea O_2 flux for model years 1980–1998 is presented in Figure 1. O_2 is taken up into the ocean in the cold tongue of the eastern equatorial Pacific, and released to the atmosphere over the remainder of the tropics. In the subtropical gyres, O_2 is outgassed except in the western boundary current regions where rapid cooling and deeper mixing occur. In the subpolar North Atlantic and Southern Ocean, significant heat loss and deep mixing drives O_2 ingassing. Zonally averaged mean fluxes compare well to the estimates of *Ganachaud and Wunsch* [2002] in all regions except the Southern Ocean. The occasional sharp meridional gradients in the O_2 flux are due to the choice of distinct regional values for $\alpha(x,y)$. A global net outgassing of 130 Tmol/yr occurs in the model, due in large part to physical stagnation in the Southern Ocean and continuing model adjustment to initial and boundary conditions. Recent studies indicate a net O_2 outgassing from the ocean in recent decades [*Keeling and Garcia*, 2002; *Plattner et al.*, 2001], with the Southern Ocean being the region where the largest changes are predicted. However, it is not readily possible to separate model drift from potential credible changes in the ocean O_2 budget and O_2 air-sea flux, and thus we remove the model mean flux and 19-year trend, and examine only interannual variability.

[6] Model estimated interannual variability of the global air-sea O_2 flux for the period 1980–1998 is presented in (Figure 2a). The air-sea O_2 flux has interannual extremes of −70 to +100 Tmol/yr, with a root-mean-square (RMS) of 35 Tmol/yr. A regional breakdown of the annual anomalies in O_2 (Figures 2b–2d) illustrates that the global flux variability is most strongly influenced by the equatorial Pacific and the North Atlantic.

[7] The relationship between air-sea heat flux and O_2 flux variations has been considered by *Keeling and Garcia* [2002] and *Plattner et al.* [2001]. In this model, temporal variability of the global mean heat flux and air-sea O_2 flux are uncorrelated (Figure 2a). However, in the North Atlantic and equatorial Pacific, correlations reflect the controlling processes. In the North Atlantic, air-sea heat and O_2 fluxes are positively correlated (r = 0.60) with slope 10.0 nmol/J, consistent with *Keeling and Garcia* [2002] (Figure 2b). In this region, heat loss is associated with deep mixing that exposes low O_2 waters to the surface and drives ocean uptake of O_2. In the equatorial Pacific, the correlation is negative (r = −0.68) because the strong upwelling of cool, oxygen depleted waters leads to a simultaneous uptake of O_2 and heat (Figure 2c).

[8] The first EOFs of air-sea O_2 fluxes in the two regions dominant to the global flux variability are presented in Figure 3. In the equatorial Pacific, EOF1 explains 73% of

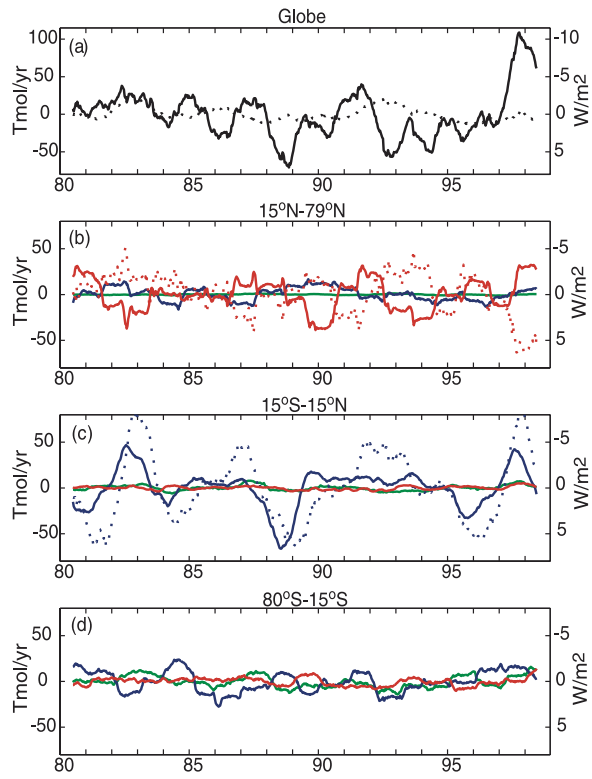

Figure 2. Solid lines are (a) globally averaged air-sea O_2 flux variability for 1980–1998, and regional averages in the Pacific (blue), Atlantic (red) and Indian (green) from (b) 15°N–79°N, (c) 15°S–15°N and (d) 80°S–15°S. Dotted lines are regional heat fluxes (positive to the ocean) for (a) the globe, (b) Atlantic, and (c) Pacific.

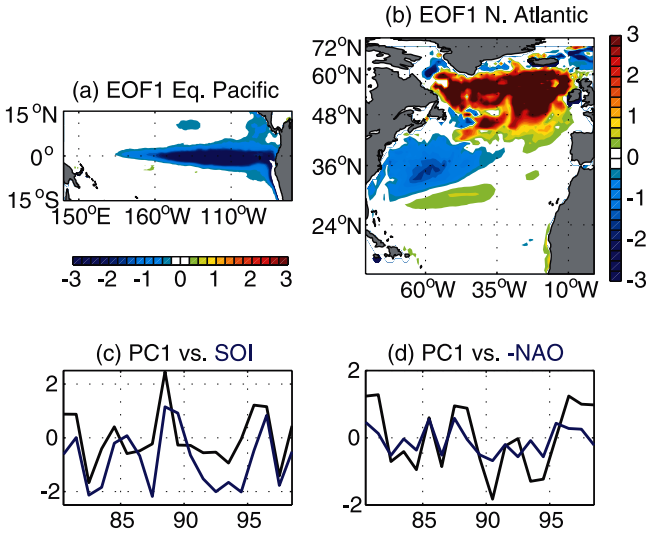

Figure 3. First Empirical Orthogonal Functions (EOF1) in mol/m^2/yr for (a) the equatorial Pacific and (b) the North Atlantic, with principle components normalized by the standard deviation (PC1) v. (c) the Southern Oscillation Index (SOI) and (d) the North Atlantic Oscillation (NAO).

the interannual variance (Figure 3a). PC1 has a maximum correlation with the SOI (r = 0.80) when the flux leads by 2 or 3 months (Figure 3c). The rapid air-sea exchange timescale for O_2 allows it to respond immediately to changes in the physical state of the equatorial Pacific, even before the atmospheric signal becomes apparent at the locations from which the SOI is observed. At zero lag, the correlation is 0.69. In the North Atlantic, EOF1 explains 28% of the interannual O_2 flux variance (Figure 3b). The maximum correlation of PC1 with the NAO (r = 0.73) occurs with no lag (Figure 3d). Similar in terms of correlation magnitude and the dipolar pattern, *Williams et al.* [2000], using another model, find that the subpolar (subtropical) convective nitrate flux is correlated at r = 0.76 (−0.59) with the NAO.

[9] ENSO impacts air-sea fluxes of O_2 in the equatorial Pacific primarily by modulating upwelling strength and the exposure of low O_2 sub-surface waters to the atmosphere. Under normal conditions in the equatorial Pacific, the thermocline shallows from west to east and strong upwelling occurs at the equator, driven by Ekman suction [*McPhaden et al.*, 1998]. This draws low oxygen waters up to the surface, resulting in the net influx of O_2 seen in Figure 1. In the El Niño phase, the thermocline in the east is depressed by eastward propagating Kelvin waves generated by anomalous westerly wind bursts in the western Pacific [*McPhaden et al.*, 1998]. At the same time, the atmospheric expression of El Niño causes slackening of the trade winds and reduced Ekman divergence at the equator. The combined effects of a depressed thermocline and reduced upwelling significantly alter the amount of low O_2 waters exposed to the atmosphere. Air-sea fluxes of O_2 experience a positive anomaly in the region of the sharp equatorial tongue (less O_2 removed from the atmosphere). In the La Niña phase, the upward slope of the thermocline to the east is enhanced, both bringing low O_2 waters closer to the surface and increasing the efficiency of divergence-driven upwelling along the equator. This results in a negative O_2 flux anomaly.

[10] Convection is the dominant forcing for O_2 flux variability in the middle and high latitudes of the North Atlantic, consistent with the regional study of *McKinley et al.* [2000]. O_2 flux variability results from a disequilibrium between summertime biological O_2 production, driven by wintertime convective nutrient supply, and the wintertime drawdown of O_2, also driven by convection [*Bender et al.*, 1996; *Keeling et al.*, 1993]. This model suggests that year-to-year imbalances between these convective and biological mechanisms drive a significant air-sea flux variability. Changes in air-sea heat fluxes and storm tracks associated with the NAO drive the dominant dipolar structure of convective variability in the North Atlantic region [*Dickson et al.*, 1996] as seen in Figure 3b. The NAO increases convection in the subpolar (subtropical) region and decreases convection in the subtropical (subpolar) in its high (low) phase. However, subpolar variability dominates the sign of the regional air-sea flux anomaly because convective changes are of a far greater magnitude than in the subtropics.

[11] We now modify equation (2) to account for modeled air-sea O_2 flux variability: $\Delta O_2 = \alpha_F F - \alpha_B B - O_2'$. Here O_2' is the interannual variability of the air-sea O_2 flux, observed as a change in O_2/N_2 in the atmosphere. To derive the atmospheric O_2/N_2 variability, air-sea N_2 flux variability is estimated using model heat fluxes and equation 19 of *Keeling et al.* [1993]. Atmospheric O_2/N_2 is then simulated with this flux and the O_2 flux as lower boundary conditions on the Geophysical Fluid Dynamics Laboratory Global Chemical Transport Model (GFDL/GCTM), with a horizontal resolution of 265 km (equal-area grids) and 11 sigma levels (following surface topography) [*Mahlman and*

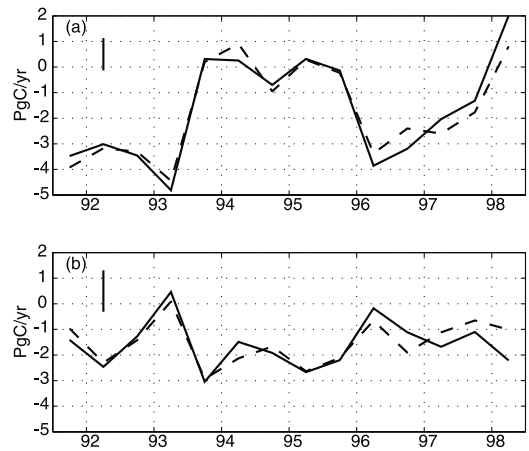

Figure 4. Estimate of (a) land and (b) ocean CO_2 sinks, with (solid) and without O_2' (dashed). Fossil fuel data (F) are global emission estimates from *Marland et al.* [2001]; and CO_2 and O_2/N_2 atmospheric observations from Alert, La Jolla, and Cape Grim (A. Manning, p. communication). O_2' is variability in O_2/N_2 retrieved from the atmospheric model at the same locations. Data and model results are averaged over 12 months, centered on April 1 and October 1 of each year. Error bars are ±0.63 PgC/yr for the land sink and ±0.81 PgC/yr for the ocean sink, based on error estimates for α_F (±0.04 PgC/yr), α_B (±0.05 PgC/yr), and F (±0.38 PgC/yr) from [*Manning*, 2001], and the impact of data sparsity (±0.5 PgC/yr) [*McKinley*, 2002].

Moxim, 1978; *Levy et al.*, 1982]. The model uses wind, temperature, and precipitation fields predicted in a general circulation model that were archived every six hours to create an annual climatology [*Manabe et al.*, 1974]. Atmospheric O_2/N_2 variability is dominated by air-sea O_2 flux variability; the N_2 flux has a small damping effect [*Keeling et al.*, 1993]. Thus, O_2' is almost entirely driven by the O_2 flux variability mechanisms discussed above.

[12] In Figure 4, the land and ocean carbon sinks calculated with and without O_2' are shown. Differences between the two estimates are largest during 1997–1998 when both strong El Niño conditions in the equatorial Pacific and the low phase of the NAO cause a positive O_2 flux anomaly (Figure 2a). When O_2' is assumed negligible (dashed curve), this source is attributed to the land biosphere and a proportional land sink of CO_2 is inferred. With the inclusion of O_2', the estimated land CO_2 sink is approximately 1 PgC/yr smaller and the ocean sink estimate is larger by the same amount. Thus, if estimates of interannual variability in CO_2 sinks are to be made using the atmospheric O_2/N_2 method, interannual variability in the air-sea flux of O_2 should not be neglected. For October 1991 – April 1998, O_2 air-sea flux variability would create an RMS error in the interannual sink estimate of 0.53 PgC/yr.

3. Conclusions

[13] In this global model, variability in the global air-sea O_2 flux is primarily forced by temporal changes in ocean circulation and mixing associated with the ENSO cycle in the equatorial Pacific, and by convective variability in the North Atlantic. Biogeochemical parameterizations used in this study are simplified and likely to damp variability, and the circulation model underestimates the physical variability of the upper ocean. Thus, our estimate of O_2 flux variability for 1980–1998 (−70 to +100 Tmol/yr) is most likely a lower bound. In turn, this indicates that CO_2 sink variability estimates using the atmospheric O_2/N_2 method under the assumption of negligible air-sea O_2 flux variability could have a larger error than estimated here (±1 PgC/yr). To address this error, correlations with heat fluxes in the equatorial Pacific and North Atlantic may provide first-order flux variability approximations, but precise estimations will require additional data and improved modeling.

[14] **Acknowledgments.** We thank the JPL ECCO group for MITgcm output; C. Hill and S. Dutkiewicz for modeling help; and A. Manning for data and discussion. Computational resources were made available by Digital Equipment, Intel Corporation, and Sun Microsystems. GAM thanks NASA for the Earth System Science Fellowship (NGT5-30189). MJF is grateful for support from NOPP grant no. N00014-02-1-0370.

References

Anderson, L. A., and J. L. Sarmiento, Redfield ratios of remineralization determined by nutrient data analysis, *Global Biogeochem. Cycles*, *8*, 65–80, 1994.

Battle, M., et al., Global carbon sinks and their variability inferred from atmospheric O_2 and $\delta^{13}C$, *Science*, *287*, 2467–2470, 2000.

Bender, M., T. Ellis, P. P. Tans, R. Francey, and D. Lowe, Variability in the O_2/N_2 ratio of the southern hemisphere air, 1991–1994: Implications for the carbon cycle, *Global Biogeochem. Cycles*, *10*, 9–21, 1996.

Boutin, J., and J. Etcheto, Climatology of K deduced from the satellite wind speeds, *OCMIP protocol README.sat*, 1995.

Conkright, M., et al., World Ocean Atlas 1998 CD-ROM Data Set Documentation, Tech. Rep. 15, NODC Internal Report, Silver Spring, MD, 1998.

Dickson, R., J. Lazier, J. Meinke, P. Rhines, and J. Swift, Long-term coordinated changes in the convective activity of the North Atlantic, *Prog. Oceanogr.*, *38*, 241–295, 1996.

Ganachaud, A. S., and C. Wunsch, Oceanic nutrient and oxygen transports and bounds on export production during the World Ocean Circulation Experiment, *Global Biogeochem. Cycles*, *16*(4), 1057, doi:10.1029/2000GB001333, 2002.

Keeling, R. F., R. P. Najjar, M. L. Bender, and P. P. Tans, What atmospheric oxygen measurements can tell us about the global carbon cycle, *Global Biogeochem. Cycles*, *7*, 37–67, 1993.

Keeling, R. F., S. C. Piper, and M. Heimann, Global and hemispheric CO_2 sinks deduced from changes in atmospheric O_2 concentration, *Nature*, *381*, 150–155, 1996.

Keeling, R. F., and H. Garcia, The change in oceanic O_2 inventory associated with recent global warming, *Proc. US Natl. Acad. Sci.*, *99*, 7848–7853, 2002.

Lee, T., I. Fukimori, D. Menemenlis, Z. Xing, and L. L. Fu, Effects of Indonesian throughflow on the Pacific and Indian ocean, *J. Phys. Ocean.*, *32*(5), 1404–1429, 2002.

Levy, H., II, H. Mahlman, and J. D. Moxim, Tropospheric N2O variability, *J. Geophys. Res.*, *87*, 3061–3080, 1982.

Mahlman, J. D., and W. J. Moxim, Tracer simulation using a global general circulation model: Results from a midlatitude instantaneous source experiment, *J. Atmos. Sci.*, *35*, 1340–1374, 1978.

Manabe, S., D. G. Hahn, and J. L. Holloway Jr., The seasonal variation of the tropical circulation as simulated by a global model of the atmosphere, *J. Atmos. Sci.*, *31*, 43–83, 1974.

Manning, A. C., Temporal variability of atmospheric oxygen from both continuous measurements and a flask sampling network: Tools for studying the global carbon cycle, Ph.D. thesis, University of California, San Diego, 2001.

Marland, G., T. A. Boden and R. J. Andres, Global, Regional, and National Annual CO_2 Emissions from Fossil-Fuel Burning, Cement Production, and Gas Flaring: 1751–1998, in Trends: A Compendium of Data on Global Change, Tech. rep., CDIAC, Oak Ridge National Laboratory, U.S. Department of Energy, Oak Ridge, Tenn. USA, 2001.

Marshall, J. C., C. Hill, L. Perelman, and A. Adcroft, Hydrostatic, quasi-hydrostatic and non-hydrostatic ocean modeling, *J. Geophys. Res.*, *102*, 5733–5752, 1997a.

Marshall, J. C., A. Adcroft, C. Hill, L. Perelman, and C. Heisey, A finite volume, incompressible Navier-Stokes model for studies of the ocean on parallel computers, *J. Geophys. Res.*, *102*, 5753–5766, 1997b.

McKinley, G. A., M. J. Follows, and J. Marshall, Interannual variability of the air-sea flux of oxygen in the North Atlantic, *Geophys. Res. Let.*, *27*, 2933–2936, 2000.

McKinley, G. A., Interannual variability of air-sea fluxes of carbon dioxide and oxygen, Ph.D. thesis, Massachusetts Institute of Technology, 2002.

McPhaden, M. J., et al., The Tropical Ocean-Global Atmosphere observing system: A decade of progress, *J. Geophys. Res.*, *103*(C7), 14,169–14,2400, 1998.

Plattner, G. K., F. Joos, and T. F. Stocker, Revision of the global carbon budget due to changing air-sea oxygen fluxes, *submitted to Global Biogeochem Cycles*, 2001.

Wanninkhof, R., Relationship between wind speed and gas exchange over the ocean, *J. Geophys. Res.*, *97*, 7373–7382, 1992.

Weiss, R. F., The solubility of nitrogen, oxygen, and argon in water and seawater, *Deep Sea Res.*, *17*, 721–735, 1970.

Williams, R. G., A. J. McLaren, and M. J. Follows, Estimating the convective supply of nitrate and implied variability in export production over the North Atlantic, *Global Biogeochem. Cycles*, *14*, 1299–1313, 2000.

G. A. McKinley, Instituto Nacional de Ecología, Periférico 5000, piso 4, C.P. 04530, México DF, México. (galen@alum.mit.edu)

M. J. Follows and J. Marshall, Department of Earth, Atmospheric and Planetary Sciences, Massachusetts Institute of Technology, Cambridge, Massachusetts, USA.

S.-M. Fan, Atmospheric and Ocean Sciences Program, Princeton University, Princeton, New Jersey, USA.